Supplementary Information

CO$_2$ forcing alone insufficient to explain Paleocene-Eocene Thermal Maximum warming

Richard E. Zeebe, James C. Zachos, and Gerald R. Dickens

NGS-2009-04-00417. Revised Version.

Submitted to *Nature Geoscience*.

June 5, 2009

1   Model description

For our simulations of the PETM, we used the **L**ong-term **O**cean-atmosphere-**S**ediment **CA**rbon cycle **R**eservoir Model (LOSCAR, see refs. 1–3), a carbon-cycle box model (modified after ref. 4), coupled to a sediment module[5]. The model includes biogeochemical cycles of total carbon, total alkalinity, phosphate, oxygen, and stable carbon isotopes. Weathering of carbonate and silicate mineral rocks is parameterized in the model as a function of atmospheric CO_2 (refs. 3,4). The model uses realistic volumes of ocean basins based on a Paleocene/Eocene topography[6]. The Atlantic, Indian, Pacific, and Tethys Ocean basins are each subdivided into surface, intermediate, and deep boxes. Prior to the PETM, deepwater formation in the model was prescribed to occur in the Southern Ocean, consistent with observations[7]. The sediment model calculates $\%CaCO_3$ (dry weight) in the bioturbated (mixed) interval of sediment as a function of rain, dissolution, burial, and chemical erosion. The thickness of this sediment layer (h_s) is typically 8 cm (see Table S1); the sediment model is more fully described elsewhere[5].

Ocean carbonate chemistry routines to calculate parameters such as $[CO_2]$, $[CO_3^{2-}]$, pH, and calcite saturation state from total CO_2 and total alkalinity use algorithms as described in ref. 8. These allow for variations in the Ca^{2+} and Mg^{2+} concentration of seawater, which most likely differed from modern values during the Paleocene/Eocene[9]. In our PETM simulations, we used $[Ca^{2+}] = 20$ mmol kg^{-1} and $[Mg^{2+}] = 30$ mmol kg^{-1}, rather than the modern values of $[Ca^{2+}] = 10$ mmol kg^{-1} and $[Mg^{2+}] = 53$ mmol kg^{-1} (ref. 9). Warmer surface and bottom water temperatures in the late Paleocene and Eocene also impact equilibrium and solubility constants. For example, the calcite saturation concentration at a bottom water temperature of $14 - 17°C$ during the PETM is quite different from the modern one at $2°C$ (see Fig. 3 of ref. 5). In the model, we used bottom water temperatures of $12°C$ and $16°C$ prior to and during the PETM, respectively (Table S1), and included the effects of changes in temperature, and $[Ca^{2+}]$ and $[Mg^{2+}]$ on the stoichiometric constants.

One important consequence of changes in oceanic $[Ca^{2+}]$ is its effect on the ocean carbon inventory. The long-term carbon inventory and carbonate chemistry of the ocean-atmosphere system is controlled by atmospheric CO_2 and the balance between riverine flux and carbonate burial[10]. Carbonate burial is tied to the deep-sea carbonate saturation, which is proportional to the product of $[Ca^{2+}] \times [CO_3^{2-}]$. If oceanic $[Ca^{2+}]$ doubles at constant saturation state, $[CO_3^{2-}]$ would be reduced by 50%. Thus, $[CO_3^{2-}]$ prior to the PETM was much lower than today if Eocene $[Ca^{2+}]$ was 20 mmol kg^{-1}. In the model, this leads to a pre-PETM ocean carbon inventory that is similar to today's value (Table S1), despite a higher baseline atmospheric CO_2 at the time.

Carbonate 'rain' to the seafloor within the model is split into two broad locations: shelf/upper slope (< 600 m) and lower slope/rise/plains (> 600 m). The pre-PETM ratio of shallow-to-deep carbonate rain was increased relative to the modern because sea-level was higher, which promotes shallow water marine carbonate deposition [as has been documented for the Paleocene and Early Eocene[11]]. In general, observations imply relatively less pelagic carbonate production during the early Cenozoic, which leads to a shallower CCD compared to the modern in agreement with observations (see below and ref. 9).

Several model parameters for the pre-PETM ocean and global carbon cycle are summarized in Table S1. Changes applied to the model during the PETM phase are described in the main paper.

Table S1. LOSCAR model parameter: Pre-PETM values.

Parameter	Description	Value	Unit
V_{oc}	Volume ocean	1.29×10^{18}	m^3
A_{oc}	Area ocean	3.49×10^{14}	m^2
f_{A_i}	%Area [A I P T H] [a]	[15 14 52 9 10]	%
h_L	Thickn. Low.-lat. surf.	100	m
h_H	Thickn. High.-lat. surf.	250	m
h_I	Thickn. interm. boxes	900	m
T	Temperature [L I D H] [b]	[25 16 12 12]	°C
THC	Conveyor circulation	25	[c] Sv
M_{oc}^C	Ocean C inventory	34,000	Pg C
M_{sed}^C	Sediment C inventory	620	Pg C
F_{in}	$CaCO_3$ riverine flux	16×10^{12}	mol C y^{-1}
h_s	Thickn. sediment mixed layer	0.08	m
ρ_s	Density, sediment solids	2.50×10^3	kg m^{-3}
n_{Si}	Silc. weathering param. [d]	0.2	—
n_C	Carb. weathering param. [d]	0.4	—

[a] Atlantic, Pacific, Indic, Tethys, and High-Latitude %Area (ref. 6).

[b] Low-Lat., Intermediate, Deep, and High-Lat. temperature.

[c] 1 Sv = 10^6 m^3 s^{-1}.

[d] See ref. 3.

2   Mass and isotopic composition of carbon input

As pointed out in the main paper, the stable carbon isotope (δ^{13}C) records alone are insufficient to determine mass and δ^{13}C-value of the carbon input. The mass balance for total carbon and stable isotopes in the combined ocean-atmosphere-biosphere system after the input reads:

$$M_f \;=\; M_i + M_s \tag{1}$$

$$R_f \times M_f \;=\; R_i \times M_i + R_s \times M_s \tag{2}$$

where M_j's are masses of carbon (in Pg C) and R_j's are ^{13}C/^{12}C ratios of the final (f) and initial (i) inventory, and of the carbon source (s). Given an initial inventory plus initial and final δ^{13}C-value, we are left with two equations [(1)$-$(2)] and three unknowns (M_f, M_s, R_s). In other words, either the input mass or its isotopic composition are still needed to solve the system. We have used deep-sea carbonate dissolution records to determine the input mass; its δ^{13}C-value is then set by eqn. (2).

3   Model sensitivity to carbon release time

Our results presented in the main paper suggest a maximum initial carbon input of ~ 3000 Pg C. We have tested whether this estimate is sensitive to the time scale of carbon input (Fig. S1). In other words, if the carbon was released over a different period of time, would this allow for a different amount of carbon input? Because we are only interested here in the relative response to the duration of the initial input pulse, the continuous release and changes in ocean circulation (see main paper) have been omitted. In the following, we will discuss scenarios in which the release time was varied, while the total input (3000 Pg C) and its isotopic composition (δ^{13}C $= -50‰$) were held constant. Other scenarios could include a larger input of isotopically heavier carbon over a longer time interval. However, this would lead to a slow and gradual CCD shoaling, which is at odds with observations.

A release time of $\sim 1,000$ y would have produced an initial, short-lived δ^{13}C-
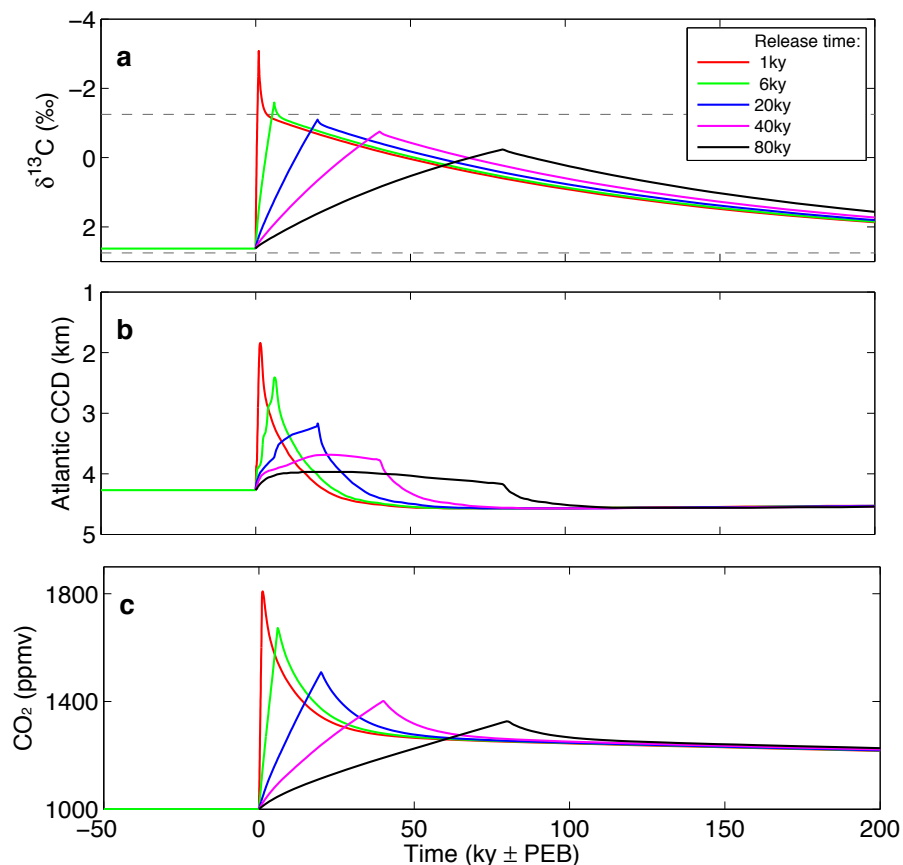
Figure S1. Model response to the release time of carbon input. Total carbon input is 3000 Pg C at $\delta^{13}C = -50‰$, deep Atlantic injection is 40%. The continuous carbon release and changes in ocean circulation (see manuscript) have been omitted here for clarity.

drop of almost 6‰ in surface ocean TCO_2. We are not aware of carbonate $\delta^{13}C$-data supporting this scenario as sites with little or no carbonate dissolution did not record such a $\delta^{13}C$-drop. Input times of $\sim 1,000$ y therefore appear unlikely, unless all carbonates that could have recorded such extreme values are absent from the records as a result of dissolution.

Increasing the release time (t_R) from 6 to 40 ky results in a moderate decrease of the maximum CIE by about 0.5‰ (Fig. S1a). However, at $t_R = 40$ ky, the CCD shoaling is too weak compared to observations. For example, the reconstructed CCD shoaling in the Atlantic is > 2 km (ref. 12), while the model predicts less than 600 m for release times longer than 40 ky (Fig. S1b). In summary, stretching the duration

of the carbon input would allow for a slightly higher carbon input at the same CIE. However, the implications for changes in the CCD appear inconsistent with the data.

4   The CCD before and during the PETM

Based on available %$CaCO_3$ records across the Upper Paleocene and Lower Eocene sediment sections from around the globe (Table S2), we have estimated the initial position and changes in the calcite compensation depth (CCD) before and during the PETM in the different ocean basins (Fig. S2).

Table S2. Sites included in CCD reconstruction.

Basin	Leg	Location	Site
Atlantic	208	Walvis Ridge	1262 1263 1265 1266 1267
Southern Ocean	113	Maud Rise	690
Indian	27	Perth Abyss. Plain	259
Indian	121	Broken Ridge	752
Pacific	198	Shatsky Rise	1208 1209 1210 1211 1212
Pacific	199	Central EqPac	1215 1220 1221

Sites at Walvis Ridge in the south-central Atlantic have been discussed in detail before[5,12] and indicate a dramatic CCD shoaling during the event by more than 2 km: from below 3.6 km prior to the event (Site 1262) to less than 1.5 km (Site 1263) during the PETM main phase (Fig. S2, blue bars). The pre-event carbonate content of ∼80% at Site 1262 indicates a CCD deeper than 3.6 km in the south-central Atlantic prior to the event. This is consistent with the lower limit of earlier CCD reconstructions for the South Atlantic, based on the absence/presence of $CaCO_3$ in a variety of deep-sea cores[13]. In general, the Atlantic records suggest a pre-event CCD shallower than ∼4 km (Fig. S5, refs. 13,14).

Southern Ocean Site 690 (paleowater depth ∼ 2100 m) has also extensively been discussed in the literature. %$CaCO_3$ drops from initial 80% to around 60% (refs. 15,16). No clay layers comparable to those at Walvis Ridge are present. Site 690 was
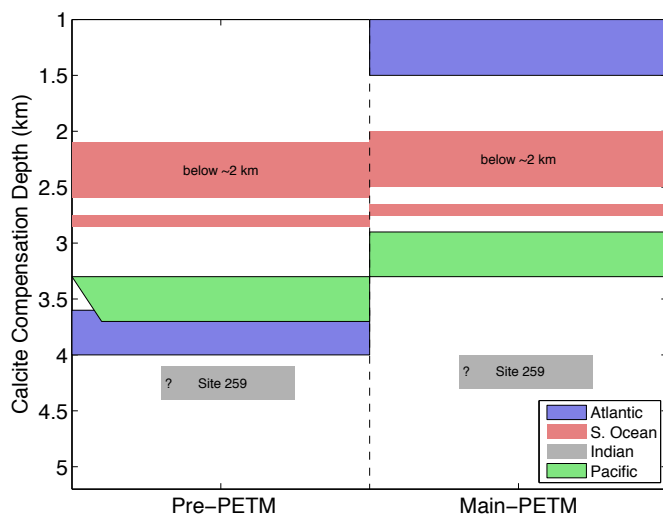
Figure S2. Position of the CCD before and during the PETM main event, based on available sediment records. The Southern Ocean CCD reconstruction is based on Site 690, which was located above the CCD before, during, and after the event. This only constrains the upper limit (below ~ 2 km) but not the lower limit (red bars).

located above the CCD before, during, and after the event. This indicates that the CCD in the Southern Ocean was below ~ 2 km prior to the event, while the %$CaCO_3$ drop at Site 690 indicates a slight CCD shoaling during the event (Fig. S2, red bars). Note that the CCD shoaling in the Southern Ocean must have been much less pronounced than in the Atlantic. At similar initial %$CaCO_3$ $(80-90\%)$ but shallower paleowater depth $(\sim 1.5$ km), %$CaCO_3$ at Atlantic Site 1263 drops to zero during the PETM, while %$CaCO_3$ at the deeper Site 690 $(\sim 2$ km) only drops to $\sim 60\%$.

Carbonate records across the PETM in the Indian Ocean are sparse. We focus here on Sites 259 (Perth Abyssal Plain) and 752 (Broken Ridge)[17,18]. The paleowater depth of Site 259 during the PETM was probably > 4000 m (see Fig. 9 in ref. 17). Fig. S3a shows measured %$CaCO_3$ at Site 259 across the PETM[17]. The sampling interval across the P/E boundary was ~ 10 cm and could have missed an interval of minimum %$CaCO_3$. Nevertheless, the three samples taken across the boundary (corresponding to the carbon isotope excursion, CIE) have values of $40-80\%$ $CaCO_3$. This is surprisingly high, given a paleowater depth of about 4 km. Site 259 could be a specific location and may not be representative for the average Indian Ocean before
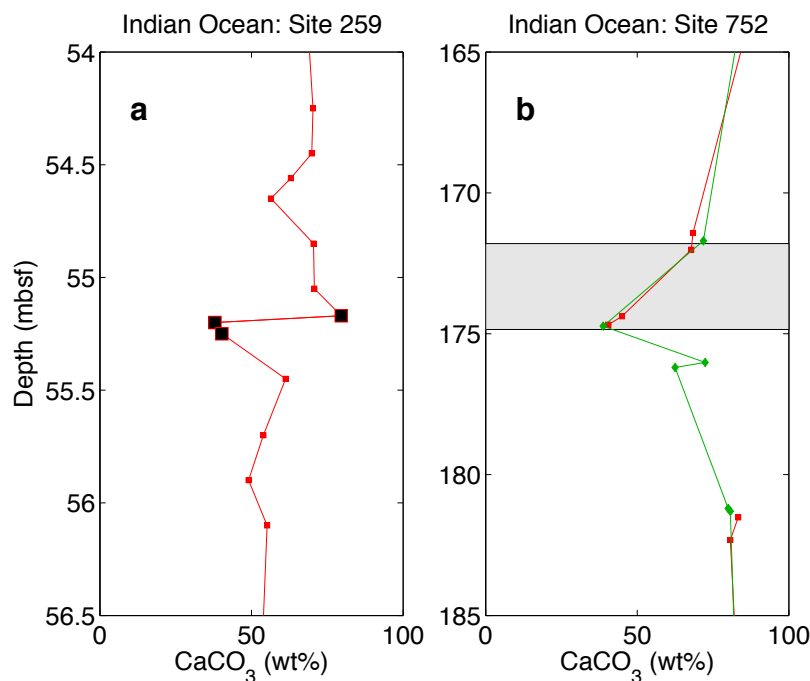
Figure S3. Records of %CaCO$_3$ at Sites 259 and 752. (a) Site 259: black squares indicate values assigned to the PETM by ref. 17. (b) Site 752: red squares (Micah Nicolo, unpublished); green diamonds: Leg 121 Shipboard Scientific Party [18]. Shaded area indicates P/E boundary interval based on benthic foraminifera [19].

and during the PETM. Nevertheless, the apparent absence of an extensive dissolution layer at this paleowater depth indicates a very minor CCD shoaling.

Indian Ocean Site 752 is located on Broken Ridge. Fig. 9 in ref. 18 indicates a lower bathyal/abyssal paleowater depth during the PETM but the paleowater depth of Site 752 during the PETM seems not well constrained (about $1-2$ km). Nevertheless, the available %CaCO$_3$ data indicate that the main event-CCD did not shoal above this depth. In summary, if the minimum %CaCO$_3$ intervals at sites 259 and 752 have not been missed by the data sampling, then the CCD shoaling in the Indian Ocean (Fig. S2, gray bars) was much less severe (as seems to be the case in the Pacific and Southern Ocean) than in the Atlantic.

Information on the position of the Pacific CCD before and during the PETM is available from Leg 198 (Shatsky Rise, Sites 1208-1212) and Leg 199 (Sites 1215, 1220, 1221). Modern and paleowater depth of Site 1208 is/was $\sim$ 3.3 km. Based

on available data, 1208 was located above (very close to) the CCD before, during, and after the event[20]. Although there are no foraminifera in PETM sediments, the most robust nannofossils are preserved, showing that Site 1208 was not below the CCD during the PETM[20]. This indicates that the CCD at this site was close to ~ 3.5 km before the event and only slightly shallower during the event. None of the Sites 1209-1212 shows any dramatic drop in %$CaCO_3$ during the main event, i.e. throughout the duration of the CIE[20]. At the shallower Sites 1209 and 1210 (paleowater depth 2400 and 2600 m), %$CaCO_3$ drops from $> 90\%$ to about 85%. At the deeper Sites 1212 and 1211 (paleowater depth 2600/2900 m), %$CaCO_3$ drops from $> 90\%$ to 70-80%. This indicates that during the main event, the CCD at Shatsky rise did not shoal above 2.9 km and was probably located close to 3.3 km (Site 1208).

Colosimo et al.[20] note an extremely thin (1 mm) dark brown clay seam within the PETM section in several locations at Shatsky Rise. This could indicate a CCD shoaling above the Shatsky Rise depth range for a very short interval at the onset of the event (for example, 1-2 k.y.), but leaving no substantial clay layer due to bioturbation. Alternatively, the clay seam may indicate the absence of carbonate rain during that interval. Irrespective of the reason, Figs. F5-F8 in ref. 20 show that a 1 mm layer would represent a very small portion $(0.5 - 1\%)$ of the section covering the total CIE, which extends over 10 to 20 cm at sites 1209-1212. Furthermore, the inferred minor CCD shoaling at Shatsky Rise throughout the main event is consistent with the data obtained during Pacific Leg 199 (see below).

Site 1220 (Leg 199) is located in the Central Equatorial Pacific, the paleowater depth during PETM was ~ 2900 m. Calcium wt% has been measured[21] from which %$CaCO_3$ has been calculated (see Geochemistry, p. 20, in Explanatory Notes chapter of Leg 199 in ref. 21). Throughout the PETM, %$CaCO_3$ in 1220 remains at about 20% (Fig. S4a). Neither %Ca nor %$CaCO_3$ drop to zero anywhere within the PETM section. This suggests that Site 1220 at ~ 2900 m paleowater depth in the tropical Pacific was located above the CCD before and during the main PETM interval.

Note that Site 1220 shows several intervals of laminations (see Fig. F4, Site 1220
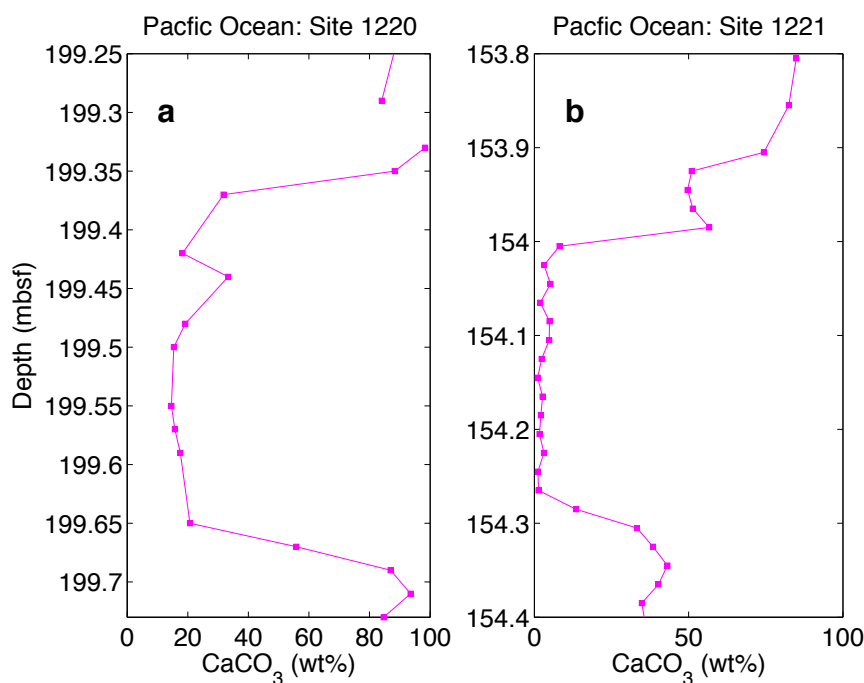
Figure S4. Records of %CaCO$_3$ at Sites 1220 (a) and 1221 (b).

in ref. 21). Bioturbation, which has been suggested to explain the lack of clay layers at the Shatsky Rise sites[20], can therefore be ruled out at Site 1220. Thus, bioturbation can not explain the observed 20% CaCO$_3$ and the absence of significant clay layers at Site 1220 during the PETM. Because all Pacific PETM sites from Leg 198 and Leg 199 show a coherent pattern of minor CCD shoaling, it is highly unlikely that the observed pattern is an artifact caused by bioturbation at all but one site (Site 1220), where bioturbation can be ruled out. Also, if the Shatsky Rise sites were strongly affected by bioturbation, then the sharp drop in δ^{13}C of bulk carbonate (same phase on which %CaCO$_3$ is measured, see Figs. F5-F8 in ref. 20) occurring over a distance of only $2-4$ cm is difficult to explain. Strong bioturbation should have destroyed the transitions.

The paleowater depth of Site 1221 during the PETM was ~ 3200 m (refs. 22,23). Measurements of %CaCO$_3$ in the PETM section are available for Hole C (Fig. S4b)[22]. The pre-PETM %CaCO$_3$ varies strongly between 20% and 80% (Fig. F1 in ref. 22),

drops close to zero during the event and increases to about 90% after the event. Relative to Site 1220, these features indicate a slightly greater paleowater depth of Site 1221 and a location very close to the CCD before the event (within the lysocline), below the CCD during, and above the CCD after the event. This suggests a pre-event CCD in the Equatorial Pacific shallower than 3500 m, consistent with other CCD reconstructions (Fig. S5, refs. 14,21).

It is important that the minimum $\%CaCO_3$ values during the PETM main phase at Site 1221 (3200 m, Equatorial Pacific) are higher than at the Walvis Ridge sites 1266 (2500 m) and 1262 (3600 m). While minimum $\%CaCO_3$ values at Site 1221 vary between 1 and 5%, all minimum values within the clay layers at sites 1266 and 1262 are 1% or less. This makes a significant difference for bottom water undersaturation[5] and is consistent with substantially less CCD shoaling at Site 1221 compared to the Walvis Ridge sites during the main event. Given the fact that $\%CaCO_3$ at Site 1220 drops to about 20% during the event (above CCD), and at Site 1221 close to 0% (below CCD), the CCD during the main PETM phase must have been located between the paleowater depths of the two sites ($2.9 - 3.3$ km).

Site 1215 is the northernmost site of Leg 199 and was probably located within the lysocline before the event. The paleowater depth during the PETM was close to that of 1221, i.e. ~ 3200 m (Fig. S5). The dissolution interval appears sharp and carbonate content drops from $60 - 80\%$ to a minimum value of about 10% (G. R. Dickens/L. Leon-Rodriguez, unpublished data). As a result, also at Site 1215, $\%CaCO_3$ did not drop to zero during the event and no clay layers comparable to those observed at Walvis Ridge appear to be present.

In summary, our compilation indicates a Pacific CCD shallower than 3500 m prior to the PETM, in agreement with other CCD reconstructions (Fig. S5, refs. 14,21). Furthermore, based on the records from Shatsky Rise and the Equatorial Pacific, the Pacific CCD shoaled only slightly during the PETM main event (Fig. S2, green bars).
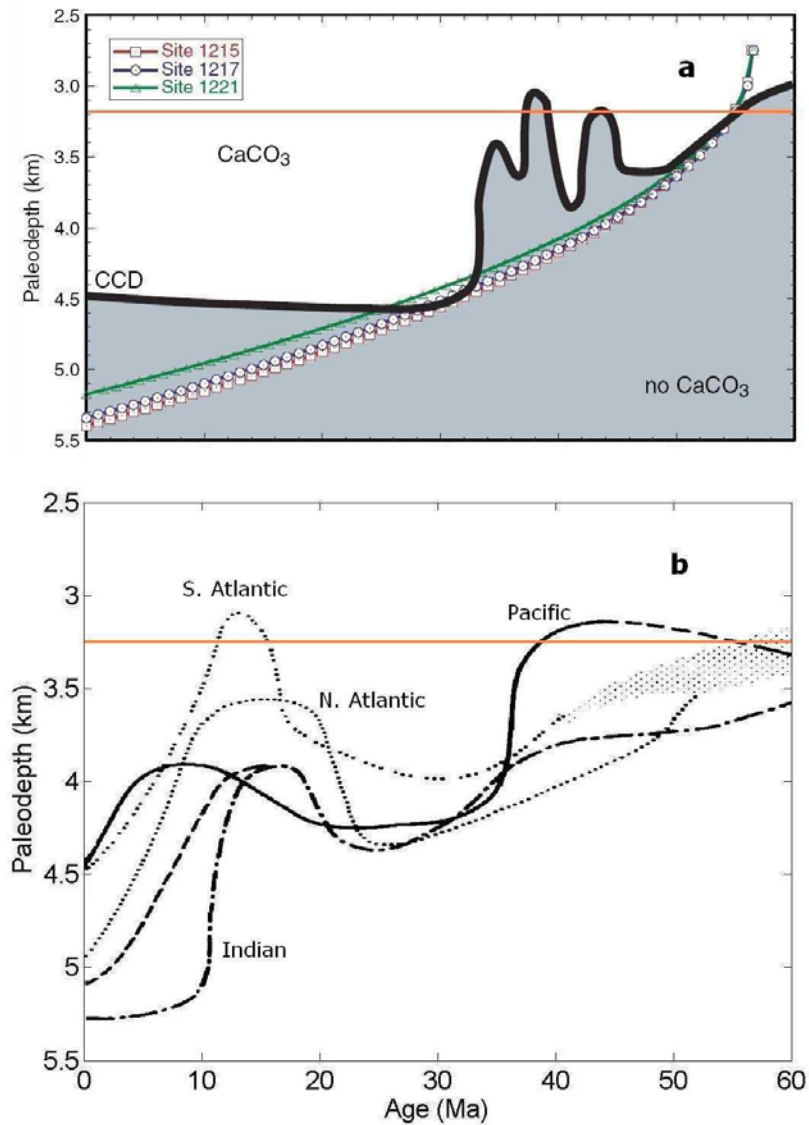
Figure S5. (a) CCD history in the Equatorial Pacific estimated by ref. 21 (see Fig. F12 in ref. 21). (b) CCD history in various ocean basins estimated by ref. 14 (see Fig. 4 in ref. 14). Orange lines indicate the position of the CCD in the (Equatorial) Pacific before the PETM.

1. Zeebe, R. E., J. C. Zachos, K. Caldeira, and T. Tyrrell. Oceans: Carbon Emissions and Acidification (in Perspectives). *Science* **321**, 51–52, doi:10.1126/science.1159124 (2008).

2. Zachos, J. C., G. R. Dickens, and R. E. Zeebe. An early Cenozoic perspective on greenhouse warming and carbon-cycle dynamics. *Nature* **451**, 279–283, doi:10.1038/nature06588 (2008).

3. Uchikawa, J., and R. E. Zeebe. Influence of terrestrial weathering on ocean acidification and the next glacial inception. *Geophys. Res. Lett.* **35**, L23608, doi:10.1029/2008GL035963 (2008).

4. Walker, J. C. G., and J. F. Kasting. Effects of fuel and forest conservation on future levels of atmospheric carbon dioxide. *Palaeogeogr. Palaeoclim. Palaeoecology* **97**, 151–189 (1992).

5. Zeebe, R. E. and J. C. Zachos. Reversed deep-sea carbonate ion basin-gradient during Paleocene-Eocene Thermal Maximum. *Paleoceanogr.* **22**, PA3201, doi:10.1029/2006PA001395 (2007).

6. Bice, K. L. and J. Marotzke. Could changing ocean circulation have destabilized methane hydrate at the Paleocene/Eocene boundary? *Paleoceanogr.* **17**, 1018, doi:10.1029/2001PA00678 (2002).

7. Thomas, D. J., T. J. Bralower, and C. E. Jones. Neodymium isotopic reconstruction of late Paleocene-early Eocene thermohaline circulation. *Earth Planet Sci. Lett.* **209**, 309–322 (2003).

8. Zeebe, R. E. and D. A. Wolf-Gladrow. *CO_2 in Seawater: Equilibrium, Kinetics, Isotopes.* Elsevier Oceanography Series, Amsterdam, (pp. 346, 2001).

9. Tyrrell, T. and R. E. Zeebe. History of carbonate ion concentration over the last 100 million years. *Geochim. Cosmochim. Acta* **68(17)**, 3521–3530 (2004).

10. Zeebe, R. E., and K. Caldeira. Close mass balance of long-term carbon fluxes from ice-core CO_2 and ocean chemistry records. *Nature Geoscience* **1**, 312–315, doi:10.1038/ngeo185 (2008).

11. Kiessling, W., Flügel, E., and Golonka, J. Patterns of phanerozoic carbonate platform sedimentation. *Lethaia* **36(3)**, 195–225 (2003).

12. Zachos, J. C., U. Röhl, S. A. Schellenberg, A. Sluijs, D. A. Hodell, D. C. Kelly, E. Thomas, M. Nicolo, I. Raffi, L. J. Lourens, H. McCarren, and D. Kroon. Rapid acidification of the ocean during the Paleocene-Eocene Thermal Maximum. *Science* **308**, 1611–1615 (2005).

13. van Andel, T. H., J. Thiede, J. G. Sclater, and W. W. Hay. Depositional history of the south atlantic ocean during the last 125 million years. *J. Geol.* **85**, 651–698 (1977).

14. van Andel, T. H. Mesozoic/Cenozoic calcite compensation depth and the global distribution of calcareous sediments. *Earth Planet. Sci. Lett.* **26**, 187–194 (1975).

15. Farley, K. A. and S. F. Eltgroth. An alternative age model for the Paleocene-Eocene thermal maximum using extraterrestrial [3]He. *Earth Planet Sci. Lett.* **208**, 135–148 (2003).

16. Kelly, D. C., J. C. Zachos, T. J. Bralower, and S. A. Schellenberg. Enhanced terrestrial weathering/runoff and surface-ocean carbonate production during the recovery stages of the Paleocene-Eocene Thermal Maximum. *Paleoceanogr.* **20**, PA4023 doi:10.1029/2005PA001163 (2005).

17. Hancock H. J. L, G. R. Dickens, E. Thomas, and K. L. Blake. Reappraisal of early Paleogene CCD curves: foraminiferal assemblages and stable carbon isotopes across the carbonate facies of Perth Abyssal Plain. *Int. J. Earth Sci. (Geol. Rundsch.)* **96**, 925–946, doi:10.1007/s00531–006–0144–0 (2007).

18. Shipboard Scientific Party. Site 752. In *Proc. ODP, Init. Repts., Vol. 121,* Weissel, J., Peirce J. et al., editor, 111–169. College Station, TX, Ocean Drilling Program, (1989).

19. Nomura, R. Paleoceanography of upper Maestrichtian to Eocene benthic foraminiferal assemblages at sites 752, 753, and 754, Eastern Indian Ocean. In *Proc. ODP, Sci. Results, Vol. 121,* Weissel, J., Peirce J. et al., editor, 3–24. College Station, TX, Ocean Drilling Program, (1991).

20. Colosimo, A. B., T. J. Bralower, and J. C. Zachos. Evidence for lysocline shoaling and methane hydrate dissociation at the Paleocene-Eocene thermal maximum on Shatsky Rise. In *Proc. ODP, Sci. Results, Vol. 198,* Bralower, T. J., Premoli Silva, I., and Malone, M. J., editor. www-odp.tamu.edu, (2005).

21. Lyle, M., P. A. Wilson, T. R. Janecek. Leg 199 summary. *Proc. ODP, Init. Repts.* **199**, 1–87 (2002).

22. Murphy, B., M. Lyle, and A. O. Lyle. Biogenic Burial across the Paleocene/Eocene Boundary: Ocean Drilling Program Leg 199 Site 1221. In *Proc. ODP, Sci. Res.,* Wilson, P. A., M. Lyle, and J. V. Firth, editor, 1–12. www-odp.tamu.edu, (2006).

23. Nunes, F. and R. D. Norris. Abrupt reversal in ocean overturning during the Palaeocene/Eocene warm period. *Nature* **439**, 60–63 (2006).